Amplified spontaneous emission and power amplification in high-power DF laser systems

Xing Chen (陈 星)*, Wenguang Liu (刘文广), and Zongfu Jiang (姜宗福)

College of Photon-Electron Science and Engineering, National University of Defense Technology, Changsha 410073, China

**E-mail: chenx04@126.com*

Received December 30, 2009

Amplified spontaneous emission (ASE) always occurs in high-power DF laser systems with master oscillator-power amplifier (MOPA) configuration. ASE not only reduces the energy extraction efficiency of the laser system, but also negatively influences its heat management. The interaction between the ASE flux and the coherent laser flux, as well as the effect of ASE on cuboid DF amplifiers, is studied using a finite difference method and an iterative arithmetic. In addition, the influence of ASE on coherent laser amplification is discussed in detail.

OCIS codes: 140.4480, 140.1550, 140.3280.

doi: 10.3788/COL20100808.0764.

The influence of amplified spontaneous emission (ASE) on high-power laser systems and laser amplifiers has been studied in a number of papers[1−4]. ASE is especially undesirable in high-gain systems because it can grow to a level at which it begins to deplete the excited populations, thereby reducing the energy extraction efficiency of the laser system.

Hunter *et al.* estimated the reduction in extraction efficiency caused by ASE in a one-dimensional steady-state amplifier[5]. In the treatment, ASE was considered as an average radiation within an average solid angle. A more detailed treatment of a similar case was conducted by Lowenthal *et al.*[6], in which ASE was calculated by a partially analytical method. Sasaki *et al.* calculated the distribution of ASE in an amplifier that had a cylindrical symmetry and small aspect ratio, and analyzed the influence of ASE on extraction efficiency[7].

In this letter, the interaction between the ASE flux and the coherent laser flux, as well as the effect of ASE on cuboid DF amplifiers, is studied using a finite difference method and an iterative arithmetic. The influence of ASE on coherent laser amplification is also discussed in detail.

To calculate the influence of ASE on energy extraction efficiency in the amplifier, the equations of ASE and the coherence laser are given. Figure 1 is the model of ASE calculations. ASE intensity at the "observation point" is obtained by integrating ASE into the entire gain media.

Assuming the light is monochromatic, ASE intensity from the emitting volume $\mathrm{d}V$ at P_0 is seen at the observation point $P(x,\, y,\, z)$ as[6,7]

$$\mathrm{d}I_{\mathrm{ASE}} = hf\frac{N^*(x_0,y_0,z_0)\mathrm{d}f}{\tau_R}\frac{\mathrm{d}V}{4\pi\left|r\right|^2}\exp\left[\int\left[g\left(l\right)-\alpha\right]\mathrm{d}l\right], \tag{1}$$

where f is the frequency of light; h is the planck constant; $N^*(x_0,\, y_0,\, z_0)$ is the upper-state population density; τ_R is the spontaneous lifetime of the upper state; r is the distance between the observation point and the emitting point; α is the nonsaturable absorption coefficient; $g(l)$ denotes the gain coefficient in the amplification with l being propagation distance in the gain media, which depends on local light intensity. By integrating Eq. (1), the total ASE intensity at P is

$$I_{\mathrm{ASE}}\left(x,y,z\right) = \iiint\left[\frac{hfN^*\left(x_0,y_0,z_0\right)}{\tau_R}\frac{\mathrm{d}V}{4\pi\left|r\right|^2}\exp\left(\int\left[g\left(l\right)-\alpha\right]\mathrm{d}l\right)\right]. \tag{2}$$

The total light intensity is the sum of ASE intensity and coherent intensity $I_f\ (x,\, y,\, z)$:

$$I\left(x,y,z\right) = \iiint\left[\frac{hfN^*\left(x_0,y_0,z_0\right)}{\tau_R}\frac{\mathrm{d}V}{4\pi\left|r\right|^2}\exp\left(\int\left[g\left(l\right)-\alpha\right]\mathrm{d}l\right)\right] + I_f\left(x,y,z\right). \tag{3}$$

For the laser light propagating along the z axis, the equation of the coherent laser flux is expressed as

$$\frac{\mathrm{d}I_f(x,y,z)}{\mathrm{d}z} = \left[g\left(x,y,z\right)-\alpha\right]I_f(x,y,z), \tag{4}$$

for which the gain coefficient is defined as

$$g\left(x,y,z\right) = \frac{g_0\left(x,y,z\right)}{1+I/I_{\mathrm{s}}}, \tag{5}$$

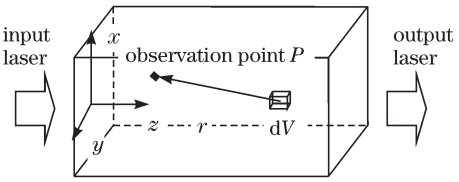

Fig. 1. Model of ASE calculations.

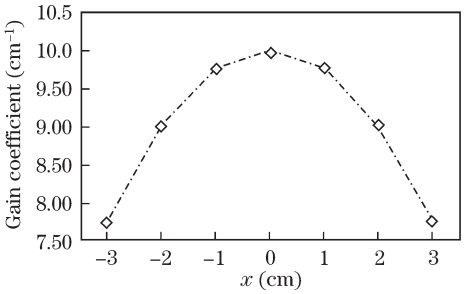

Fig. 2. Small signal gain coefficient along the x axis.

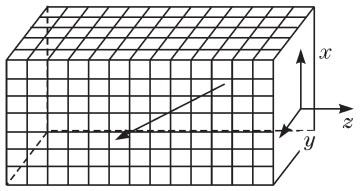

Fig. 3. Mesh configuration used in calculations.

where the saturation intensity $I_{\rm s} = \frac{h\nu}{\sigma\tau_{\rm eff}}$, $\tau_{\rm eff}$ is the effective lifetime of the upper-state population, and σ is the stimulated emission cross-section. In this letter, it is assumed that N^* is invariable and that the gain coefficient is determined by the local light intensity.

The calculation of ASE at an observation point requires summation over the entire gain media. We consider the gain media as a cuboid of length L (z axis), width D (x axis), and height H (y axis), with uniform upper-state population density, and loaded by the longitudinal coherent flux. We assume that the input coherent light is a plane wave, and the small signal gain coefficient is uniformly distributed along the z and y axes, but has a parabolic distribution along the x axis (Fig. 2)[8]. The mesh configuration used here — $7 \times 7 \times 29$ — is illustrated in Fig. 3. Spontaneous emission is considered to be emitted from the center of each element. The amplification of the light from the "emitting point" to the observation point is considered as follows: the path between these two points is divided into path elements. The gain is calculated for each path element, which is defined by the method of the nearest grid approximation, and the gain coefficient of a path element employs the value of the corresponding volume element.

The finite difference expressions for the numerical calculation of Eqs. (3) and (4) are as follows:

$$I(i_0,j_0,k_0) = \sum_i \sum_j \sum_k \left[h\nu \frac{N^*(i,j,k)}{\tau_R} \frac{{\rm d}V}{4\pi r^2} \cdot \exp\left[\sum_u (g_u - \alpha)\Delta l \right] \right] + I_f(i_0,j_0,k_0), \quad (6)$$

$$I_f(i_0,j_0,k_0) = I_f(i_0,j_0,k_0-1) \cdot \exp\left[g(i_0,j_0,k_0-1) \cdot \Delta z \right], \quad (7)$$

where i, j, k, i_0, j_0, and k_0 are corrdinate coefficients of the space lattices. $I_f = \hat{U} \cdot \hat{U}^*$; thus Eq. (7) can be converted into

$$\hat{U}_f^g(i_0,j_0,k_0) = \hat{U}_f(i_0,j_0,k_0-1) \cdot \exp[g(i_0,j_0,k_0-1) \cdot \Delta z/2], \quad (8)$$

where $\hat{U}_f(i_0,j_0,k_0)$ is the electric field after propagating $\hat{U}_f(i_0,j_0,k_0-1)$ through free space for distance Δz, and $\hat{U}_f^g(i_0,j_0,k_0)$ is the electric field after propagating $\hat{U}_f(i_0,j_0,k_0-1)$ through the gain media for distance Δz.

In the amplifier, the electric field vector $\hat{U}(x,y,z)$ satisfies the Helmholtz equation:

$$[{\rm i}2k_{\rm w}(\partial/\partial z) + \nabla_T^2]\,\hat{U}(x,y,z) = 0, \quad (9)$$

where $k_{\rm w}$ is the wave vector and $\nabla_T^2 = (\partial^2/\partial x^2 + \partial^2/\partial y^2)$ uses the following difference equation of Dufort and Frankel[8]:

$$\begin{cases} \dfrac{\partial U}{\partial z} = \frac{1}{2\Delta z}\left(U_{i_0,j_0}^{k_0+1} - U_{i_0,j_0}^{k_0-1}\right) \\ \dfrac{\partial^2 U}{\partial x^2} = \frac{1}{\Delta x^2}\left(U_{i_0+1,j_0}^{k_0} - U_{i_0,j_0}^{k_0+1} - U_{i_0,j_0}^{k_0-1} + U_{i_0-1,j_0}^{k_0}\right) \\ \dfrac{\partial^2 U}{\partial y^2} = \frac{1}{\Delta y^2}\left(U_{i_0,j_0+1}^{k_0} - U_{i_0,j_0}^{k_0+1} - U_{i_0,j_0}^{k_0-1} + U_{i_0,j_0-1}^{k_0}\right) \end{cases}, \quad (10)$$

where $x = i\triangle x$; $y = j\triangle y$; $z = k\triangle z$; $\triangle x$ and $\triangle y$ are the cell dimensions in the x and y directions, respectively. After substituting Eq. (10) into Eq. (9), we obtain the following propagation algorithm[9]:

$$\begin{aligned} U_{i_0,j_0}^{k_0+1} = {} & \frac{1}{1+\delta x^2+\delta y^2+2\delta x\delta y}[U_{i_0,j_0}^{k_0-1} + i\delta x(U_{i_0+1,j_0}^{k_0} - 2U_{i_0,j_0}^{k_0-1} + U_{i_0-1,j_0}^{k_0}) \\ & + \delta x^2(U_{i_0+1,j_0}^{k_0} - 2U_{i_0,j_0}^{k_0-1} + U_{i_0-1,j_0}^{k_0}) + \delta x\delta y(U_{i_0+1,j_0}^{k_0} - U_{i_0,j_0}^{k_0-1} + U_{i_0-1,j_0}^{k_0}) \\ & + i\delta y(U_{i_0,j_0+1}^{k_0} - 2U_{i_0,j_0}^{k_0-1} + U_{i_0,j_0-1}^{k_0}) + \delta y^2(U_{i_0,j_0+1}^{k_0} - U_{i_0,j_0}^{k_0-1} + U_{i_0,j_0-1}^{k_0}) \\ & + \delta x\delta y(U_{i_0,j_0+1}^{k_0} - U_{i_0,j_0}^{k_0-1} + U_{i_0,j_0-1}^{k_0})], \quad (k_0 = 1,2,\cdots), \end{aligned} \quad (11)$$

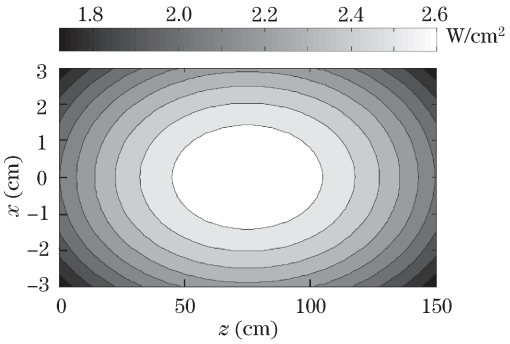

Fig. 4. ASE flux distribution with $I_{\rm in} = 0$.

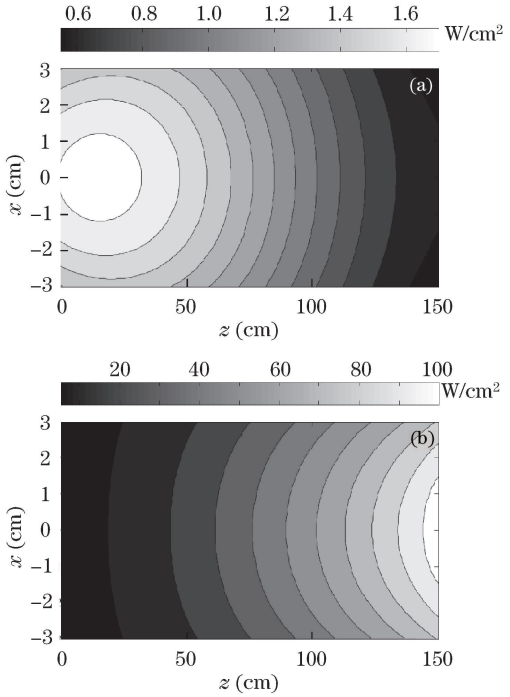

Fig. 5. (a) ASE flux distribution and (b) coherent flux distribution at $y = 0$ plane with $I_{\rm in} = 4$ W/cm^2.

where $\delta x = \triangle z/k(\triangle x)^2$ and $\delta y = \triangle z/k(\triangle y)^2$. Equation (11) enables the computation of the field at $z + \triangle z$ from the known field values at z and $z - \triangle z$.

When $k_0 = 0$, $U^1_{i_0,j_0}$ can be calculated using[10]

$$U^1_{i_0,j_0} = U^0_{i_0,j_0} + i[\delta x(U^0_{i_0+1,j_0} - 2U^0_{i_0,j_0} + U^0_{i_0-1,j_0}) + \delta y(U^0_{i_0,j_0+1} - U^0_{i_0,j_0} + U^0_{i_0,j_0-1})], \quad (12)$$

where $U^0_{i_0,j_0}$ represents the boundary condition. Equation (12) is used to propagate the complex field for the first segment, whereas Eq. (11) is used for the remaining segments.

Using Eqs. (6), (7), (8), (11), and (12), the ASE flux and the coherent flux distributions in the amplifier can be calculated based on an iterative process. When a small signal gain coefficient is given, we can calculate the initial ASE flux and coherent flux distributions; the gain coefficient is then calculated. In each step of the iteration process, the ASE flux and the coherent flux are calculated using the gain coefficient obtained from the previous step. The quantities are renewed from time to time until the convergence condition $\left\| g^{\rm new}_{i,j,k} - g_{i,j,k} \right\| < 0.01$ is reached.

In this letter, the laser wavelength $\lambda = 3.8$ μm; the upper-state population $N^* = 1.9 \times 10^{23}$ m^{-3}; the stimulated emission cross-section $\sigma = 1.7 \times 10^{-23}$ m^2; the effective lifetime of the upper-state population $\tau = 0.01$ s. After the calculation, the saturation intensity in the amplifier is about 31 W/cm^2.

Figure 4 shows the ASE flux distribution with $I_{\rm in} = 0$ and the gain length of 1.5 m. As seen in Fig. 4, the ASE flux distribution is large in the center and small around the center without the coherent light incidence on the amplifier. Figure 5 shows the ASE flux distribution and the coherent flux distribution with $I_{\rm in} = 4$ W/cm^2.

Comparing Fig. 5(a) with Fig. 4, we find that the peak value of the ASE flux transfers from the center to the forepart of the gain media, causing the magnitude of ASE to decrease. This phenomenon is caused by the gain coefficient in the amplifier decreasing along with the increase in input coherent intensity. Furthermore, the change in the gain coefficient in the forepart of the amplifier is lower than that in the back end.

Table 1 presents the data for input coherent intensity ($I_{\rm in}$), input coherent laser power ($P_{\rm in}$), extraction power ($P_{\rm out} - P_{\rm in}$), energy extraction efficiency ($E_{\rm ff}$), and amplification ratio (AR) with the gain length of 1.5 m. Here, $E_{\rm ff} = (P_{\rm out} - P_{\rm in})/P_{\rm avail}$, AR $= P_{\rm out}/P_{\rm in}$, and $P_{\rm avail} = AI_{\rm s}g_0l_{\rm g}$, $A = 0.07 \times 0.07$ (m) is the area of the gain media cross-section, $I_{\rm s}$ is the saturation intensity, and $l_{\rm g}$ is the length of the gain media. Table 1

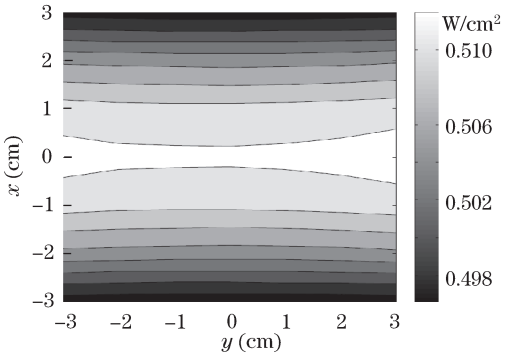

Fig. 6. ASE distribution on the plane 0.5 m away from the amplifier's exit.

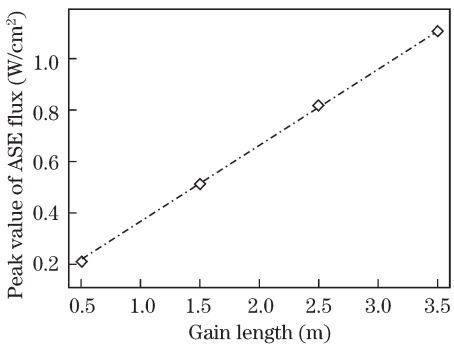

Fig. 7. Peak value of ASE as a function of gain length.

Table 1. Extraction Power, Extraction Efficiency, Amplification Ratio, and Maximum of ASE Flux for Different Input Coherent Intensities at l_g = 1.5 m

Without ASE					With ASE			
I_{in} (W/cm^2)	P_{in} (W)	$P_{out}-P_{in}$ (W)	E_{ff}	AR	$P_{out}-P_{in}$ (W)	E_{ff}	AR	ASE_{max} (W/cm^2)
1	49	3259.0	0.1600	67.51	3048.2	0.1497	63.20	2.2067
4	196	4691.3	0.2303	24.94	4549.1	0.2233	24.21	1.8257
9	441	5587.5	0.2743	13.67	5488.1	0.2694	13.44	1.5093
16	784	6237.9	0.3063	8.96	6166.4	0.3027	8.87	1.2536
25	1225	6743.6	0.3311	6.50	6690.7	0.3285	6.46	1.0508

Table 2. Extraction Power, Extraction Efficiency, Amplification Ratio, and Maximum of ASE Flux for Different Gain Lengths at P_{in} = 441 W

AR Without ASE				AR With ASE			
l_g (m)	$P_{out}-P_{in}$ (W)	E_{ff}	AR	$P_{out}-P_{in}$ (W)	E_{ff}	AR	ASE_{max} (W/cm^2)
0.5	1246.7	0.1836	3.83	1213.6	0.1787	3.75	1.2799
1.5	5587.5	0.2743	13.67	5488.1	0.2694	13.44	1.5093
2.5	10729	0.3160	25.33	10618	0.3128	25.08	1.6934
3.5	16112	0.3390	37.54	16007	0.3368	37.30	1.8797

shows that ASE influences E_{ff} and AR. Additionally, the effects decrease when the input coherent intensity increases. As seen in Table 1, the peak value of ASE flux decreases along with the increase in input coherent laser power.

Table 2 presents the data extraction power for $P_{out}-P_{in}$, E_{ff}), and AR with P_{in} = 441 W. In Table 2, the energy extraction efficiency increases along with the increase in gain length regardless of ASE. The influence of ASE on the coherent laser's AR is enhanced as gain length increases. Table 2 also indicates that the peak value of the ASE flux increases along with the increase in gain length.

The ASE radiation's heat influence on the latter optical apparatus is a problem that designers are concerned about in the master oscillator-power amplifier (MOPA) configuration. Figure 6 shows the ASE distribution (the gain length is 1.5 m) on the plane, which is 0.5 m away from the amplifier's exit. In Fig. 7, the peak value of ASE is plotted as a function of gain length. As seen in Fig. 7, the peak value of ASE is linear with gain length. The increase in gain length can induce the increase in the peak value of ASE.

In conclusion, the three-dimensional calculation technique presented in this letter enables the evaluation of ASE influence on the amplifier. The ASE flux is always large at the center without light incidence on the amplifier. ASE restrains more heavily as the intensity of the input light increases. The influence of ASE on the energy extraction efficiency of coherent lasers increases along with the increase in gain length. We also calculate the ASE distribution on the plane was 0.5 m away from the amplifier's exit. These calculation results serve as reference to designers who embark on projects using the laser system of the MOPA configuration.

References

1. N. P. Barnes and B. M. Walsh, IEEE J. Quantum Electron. **35,** 101 (1999).
2. R. H. Lehmberg and J. L. Giuliani, J. Appl. Phys. **94,** 31 (2003).
3. C. Goren, Y. Tzuk, G. Marcus, and S. Pearl, IEEE J. Quantum Electron. **42,** 1239 (2006).
4. X. Kong, X. Luo, X. Zhang, W. Zhang, and H. Li, Chinese J. Lasers (in Chinese) **30,** 385 (2003).
5. A. M. Hunter and R. O. Hunter, IEEE J. Quantum Electron. **17,** 1879 (1981).
6. D. D. Lowenthal and J. M. Eggleston, IEEE J. Quantum Electron. **22,** 1165 (1986).
7. A. Sasaki and K. Kasuya, J. Appl. Phys. **65,** 231 (1989).
8. W. Liu, "Study on the cylindrical continuous wave HF chemical high energy lasers" (in Chinese) PhD. dissertation (National University of Defense Technology, Changsha, 2004).
9. R. D. Richtmyer and K. W. Morton, *Difference Methods for Initial Value Problems* (Interscience Publishers, New York, 1967).
10. D. B. Rensch, Appl. Opt. **13,** 2546 (1974).